Inorganic Chemistry
Article

Inorg. Chem. **2010**, *49*, 5971–5976 **5971**
DOI: 10.1021/ic100518b

Efficient Synthetic Strategy to Construct Three-Dimensional 4f−5d Networks Using Neutral Two-Dimensional Layers As Building Blocks

Hu Zhou,[†,‡] Ai-Hua Yuan,[*,‡] Su-Yan Qian,[‡] You Song,[*,§] and Guo-Wang Diao[*,†]

[†]*School of Chemistry and Chemical Engineering, Yangzhou University, Yangzhou 225002, China,* [‡]*School of Material Science and Engineering, Jiangsu University of Science and Technology, Zhenjiang 212003, China, and* [§]*State Key Laboratory of Coordination Chemistry, Nanjing National Laboratory of Microstructures, School of Chemistry and Chemical Engineering, Nanjing University, Nanjing 210093, China*

Received March 18, 2010

The reaction of neutral two-dimensional (2D) layer $Tb(H_2O)_5W(CN)_8$ with pyrazine in the acetonitrile solution has led to a 3D bimetallic complex, $Tb(H_2O)_4(pyrazine)_{0.5}W(CN)_8$ (**1**). In the structure of **1**, the eight-coordinated W center adopts a slightly distorted dodecahedron, while the Tb center exhibits a nine-coordinated slightly distorted tricapped trigonal prism. The Tb^{3+} atoms and the $[W(CN)_8]^{3-}$ units are linked in alternating fashion in the *ab* crystallographic plane, resulting in an infinite 2D corrugated layers. The linear bis-monodentate pyrazine ligands acting as pillars link adjacent layers along the *c* axis to form an extended 3D open framework. The possible formation mechanism is proposed, and the temperature has played a crucial role for the formation of **1**. Magnetic measurements revealed the presence of ferromagnetic interaction between Tb^{III} and W^{V} centers. **1** marks the first structural pattern using the neutral 2D layer as building block and the first 3D complex with Ln^{III}-$[W^{V}(CN)]_8$ found in octacyanometallate-based system. Such a novel and effective building-block methodology will provide a new attractive path forward in developing functionalities of 3D 4f−5d system and may provide an opportunity to obtain 3D magnet in 4f−5d assembly.

Introduction

Cyanometallates have received much attention in the design and synthesis of new molecule-based magnets because of their intriguing molecular topologies[1] and interesting functionalities.[2−8] Recently, octacyanometallates $[M(CN)_8]^{3-/4-}$ (M = Mo, W, Nb) with higher coordination numbers have been aggressively studied.[9] The combination of the paramagnetic $[M(CN)_8]^{3-}$ (M = Mo, W) or $[Nb(CN)_8]^{4-}$ anionic species and transition-metal cations has produced various dimensional molecular structures and further displayed interesting magnetic properties, such as relatively high Curie temperatures,[10] photoinduced-magnetism,[11] and single-molecule magnetism.[12]

*To whom correspondence should be addressed. E-mail: gwdiao@yzu.edu.cn (G.-W.D.); aihuayuan@163.com (A.-H.Y.); yousong@nju.edu.cn (Y. S.).

(1) (a) Yuan, A. H.; Lu, R. Q.; Zhou, H.; Chen, Y. Y.; Li, Y. Z. *CrystEngComm* **2010**, *12*, 1382–1384. (b) Dong, W.; Zhu, L. N.; Sun, Y. Q.; Liang, M.; Liu, Z. Q.; Liao, D. Z.; Jiang, Z. H.; Yan, S. P.; Cheng, P. *Chem. Commun*. **2003**, 2544–2545.

(2) (a) Ferlay, S.; Mallah, T.; Ouahes, R.; Viellet, P.; Verdaguer, M. *Nature* **1995**, *378*, 701–703. (b) Entley, W. R.; Girolami, G. S. *Science* **1995**, *268*, 397–400. (c) Manriquez, J. M.; Yee, G. T.; McLean, R. S.; Epstein, A. J.; Miller, J. S. *Science* **1991**, *252*, 1415–1417.

(3) (a) Sato, O.; Iyoda, T.; Fujishima, A.; Hashimoto, K. *Science* **1996**, *272*, 704–705. (b) Sato, O.; Iyoda, T.; Fujishima, A.; Hashimoto, K. *Science* **1996**, *271*, 49–51.

(4) Agusti, G.; Cobo, S.; Gaspar, A. B.; Molnar, G.; Moussa, N. O.; Szilagyi, P. A.; Palfi, V.; Vieu, C.; Munoz, M. C.; Real, J. A.; Bousseksou, A. *Chem. Mater*. **2008**, *20*, 6721–6732.

(5) (a) Nilchi, A.; Malek, B.; Maragheh, M. G.; Khanchi, A. *J. Radioanal. Nucl. Chem*. **2003**, *258*, 457–462. (b) Ayrault, S.; Jimenez, B.; Garnier, E.; Fedoroff, M.; Jones, D. J.; Loss-Neskovic, C. *J. Solid State Chem*. **1998**, *141*, 475–485. (c) Dunbar, K. R.; Heintz, R. A. *Prog. Inorg. Chem*. **1997**, *45*, 283–391. (d) Kuyper, J.; Boxhoorn, G. *J. Catal*. **1987**, *105*, 163–171.

(6) (a) Larionova, J.; Guari, Y.; Blanc, C.; Dieudonné, P.; Tokarev, A.; Guérin, C. *Langmuir* **2009**, *25*, 1138–1147. (b) Baioni, A. P.; Vidotti, M.; Fiorito, P. A.; Ponzio, E. A.; de Torresi, S. I. C. *Langmuir* **2007**, *23*, 6796–6800.

(7) (a) Yuan, A. H.; Chu, C. X.; Zhou, H.; Yuan, P.; Liu, K. K.; Li, Li.; Zhang, Q. F.; Chen, X.; Li, Y. Z. *Eur. J. Inorg. Chem*. **2010**, 866–871. (b) Culp, J. T.; Smith, M. R.; Bittner, E.; Bockrath, B. *J. Am. Chem. Soc*. **2008**, *130*, 12427–12434. (c) Hartman, M. R.; Peterson, V. K.; Liu, Y.; Kaye, S. S.; Long, J. R. *Chem. Mater*. **2006**, *18*, 3221–3224. (d) Kaye, S. S.; Long, J. R. *J. Am. Chem. Soc*. **2005**, *127*, 6506–6507.

(8) (a) Goodwin, A. L.; Kennedy, B. J.; Kepert, C. J. *J. Am. Chem. Soc*. **2009**, *131*, 6334–6335. (b) Goodwin, A. L.; Calleja, M.; Conterio, M. J.; Dove, M. T.; Evans, J. S. O.; Keen, D. A.; Peters, L.; Tucker, M. G. *Science* **2008**, *319*, 794–797. (c) Chapman, K. W.; Chupas, P. J.; Kepert, C. J. *J. Am. Chem. Soc*. **2005**, *127*, 15630–15636. (d) Margadonna, S.; Prassides, K.; Fitch, A. N. *J. Am. Chem. Soc*. **2004**, *126*, 15390–15391.

(9) (a) Przychodzeń, P.; Korzeniak, T.; Podgajny, R.; Sieklucka, B. *Coord. Chem. Rev*. **2006**, *250*, 2234–2260. (b) Sieklucka, B.; Podgajny, R.; Przychodzeń, P.; Korzeniak, T. *Coord. Chem. Rev*. **2005**, *249*, 2203–2221. (c) Larionova, J.; Willemin, S.; Donnadieu, B.; Henner, B.; Guérin, C.; Gillon, B.; Goujon, A. *J. Phys. Chem. Solids* **2004**, *65*, 677–691. (d) Sieklucka, B.; Podgajny, R.; Przychodzeń, P.; Kania, R. *C. R. Chim*. **2002**, *5*, 639–649. (e) Garde, R.; Desplanches, C.; Bleuzen, A.; Veillet, P.; Verdaguer, M. *Mol. Cryst. Liq. Cryst*. **1999**, *334*, 587–595.

© 2010 American Chemical Society
Published on Web 06/09/2010

A variety of synthetic strategies have been employed to construct $[M(CN)_8]^{3-/4-}$ (M = Mo, W, Nb)-based heterometallic complexes, including the direct combination of molecular precursors,[13] the use of secondary reagent and assisting molecules,[14] employ of bridging spacers,[10e,15] clusters as building block,[16] along with the electrochemical synthesis.[11d] However, the development of octacyano- and lanthanide-based heterobimetallic assemblies has been somewhat hampered by the tendency of the lanthanide ions to adopt higher coordination numbers, their ability to easily adapt to a given environment, and in the absence of design strategies for 4f−*n*d (*n* = 3−5) networks. As far as we know, limited examples of octacyano- and lanthanide-based complexes have been reported to date.[17] For instance, Sieklucka et al. has synthesized and characterized a family of two-dimensional (2D) layers of the general formula $Ln(H_2O)_5M(CN)_8$ (Ln = Eu, Tb, Sm, Gd; M = Mo, W).[17f,j] In particular, the $Tb(H_2O)_5W(CN)_8$ presents long-range magnetic ordering below 2.8 K, and the presence of luminescence along with ferromagnetic ordering suggests that this material may be identified as a bifunctional coordination complex,[17j] exhibiting diverse physical responses when subjected to various external stimuli. It is should be mentioned here that the interlayer distance between coordinated oxygen atoms of water molecules in the structure of the complex is about 3.9−6.1 Å, which offers an opportunity for the layers to incorporate appropriate pillared ligand, thus generating a 3D open framework. This would modify the magnetic properties of the original layered system.

Along this line and the building-block methodology of Hofmann system,[18] we performed the reaction between neutral 2D layers $Tb(H_2O)_5W(CN)_8$ and pillared ligand pyrazine in the acetonitrile solution. Excitingly, a novel 3D heterometallic complex $[Tb(H_2O)_4(pyrazine)_{0.5}]W(CN)_8$ (**1**) has been obtained, which presents the first example of octacyanometallate-based assemblies using neutral 2D layers as building block. To our knowledge, **1** is also the first 3D cyanide-based complexes including lanthanide ions and octacyanotungstate(V) group, which may provide an opportunity to obtain 3D magnet in 4f−5d assembly. In this article, we present its synthesis, crystal formation mechanism, crystal structure, and magnetic properties.

Experimental Section

Synthesis. Unless otherwise mentioned, all reactants were used as purchased without further purification. Single crystals of **1** were obtained as follows: $Tb(NO_3)_3.6H_2O$ (0.05 mmol) and $[HN(n\text{-}C_4H_9)_3]_3[W(CN)_8]\cdot 4H_2O$[19] (0.05 mmol) were both added to a large vial (15 mL), in which a smaller vial (3 mL) containing pyrazine (0.15 mmol) was placed. Then, acetonitrile was carefully layered above solids and the large vial was sealed.

(10) (a) Kosaka, W.; Imoto, K.; Tsunobuchi, Y.; Ohkoshi, S. *Inorg. Chem.* **2009**, *48*, 4604–4606. (b) Pinkowicz, D.; Podgajny, R.; Baanda, M.; Makarewicz, M.; Gawe, B.; Łasocha, W.; Sieklucka, B. *Inorg. Chem.* **2008**, *47*, 9745–9747. (c) Herrera, J. M.; Franz, P.; Podgajny, R.; Pilkington, M.; Biner, M.; Decurtins, S.; Stoeckli-Evans, H.; Neels, A.; Garde, R.; Dromzée, Y.; Julve, M.; Sieclucka, B.; Hashimoto, K.; Okhoshi, S.; Verdaguer, M. *C. R. Chim.* **2008**, *11*, 1192–1199. (d) Kosaka, W.; Hashimoto, K.; Ohkoshi, S. *Bull. Chem. Soc. Jpn.* **2008**, *81*, 992–994. (e) Podgajny, R.; Pinkowicz, D.; Korzeniak, T.; Nitek, W.; Rams, M.; Sieklucka, B. *Inorg. Chem.* **2007**, *46*, 10416–10425. (f) Ohkoshi, S.; Tsunobuchi, Y.; Takahashi, H.; Hozumi, T.; Shiro, M.; Hashimoto, K. *J. Am. Chem. Soc.* **2007**, *129*, 3084–3085. (g) Higashikawa, H.; Okuda, K.; Kishine, L.; Masuhara, N.; Inoue, K. *Chem. Lett.* **2007**, *36*, 1022–1023. (h) Withers, J. R.; Li, D. F.; Triplet, J.; Ruschman, C.; Parkin, S.; Wang, G. B.; Yee, G. T.; Holmes, S. M. *Inorg. Chem.* **2006**, *45*, 4307–4309. (i) Song, Y.; Ohkoshi, S.; Arimoto, Y.; Seino, H.; Mizobe, Y.; Hashimoto, K. *Inorg. Chem.* **2003**, *42*, 1848–1856. (j) Zhong, J. Z.; Seino, H.; Mizobe, Y.; Hidai, M.; Verdaguer, M.; Ohkoshi, S.; Hashimoto, K. *Inorg, Chem.* **2000**, *39*, 5095–5101.

(11) (a) Zhao, H. H.; Shatruk, M.; Prosvirin, A. V.; Dunbar, K. R. *Chem.—Eur. J.* **2007**, *13*, 6573–6589. (b) Ohkoshi, S.; Ikeda, S.; Hozumi, T.; Kashiwagi, T.; Hashimoto, K. *J. Am. Chem. Soc.* **2006**, *128*, 5320–5321. (c) Mathonière, C.; Podgajny, R.; Guionneau, P.; Labrugere, C.; Sieklucka, B. *Chem. Mater.* **2005**, *17*, 442–449. (d) Hozumi, T.; Hashimoto, K.; Ohkoshi, S. *J. Am. Chem. Soc.* **2005**, *127*, 3864–3869. (e) Herrera, J. M.; Marvaud, V.; Verdaguer, M.; Marrot, J.; Kalisz, M.; Mathonière, C. *Angew. Chem., Int. Ed.* **2004**, *43*, 5468–5471. (f) Arimoto, Y.; Ohkoshi, S.; Zhong, Z. J.; Seino, H.; Mizobe, Y.; Hashimoto, K. *J. Am. Chem. Soc.* **2003**, *125*, 9240–9241.

(12) (a) Hilfiger, M. G.; Zhao, H. H.; Prosvirin, A.; Wernsdorfer, W.; Dunbar, K. R. *Dalton Trans.* **2009**, 5155–5163. (b) Lim, J. H.; Yoon, J. H.; Kim, H. C.; Hong, C. S. *Angew. Chem., Int. Ed.* **2006**, *45*, 7424–7426. (c) Song, Y.; Zhang, P.; Ren, X. M.; Shen, X. F.; Li, Y. Z.; You, X. Z. *J. Am. Chem. Soc.* **2005**, *127*, 3708–3709.

(13) (a) Wang, Y.; Wang, T. W.; Xiao, H. P.; Li, Y. Z.; Song, Y.; You, X. Z. *Chem.—Eur. J.* **2009**, 7648–7655. (b) Yuan, A. H.; Liu, W. Y.; Zhou, H.; Chen, Y. Y.; Shen, X. P. *J. Mol. Struct.* **2009**, *919*, 356–360. (c) Yuan, A. H.; Liu, W. Y.; Zhou, H.; Qian, S. Y. *J. Coord. Chem.* **2009**, *62*, 3592–3598. (d) Wang, Z. X.; Li, X. L.; Liu, B. L.; Tokoro, H.; Zhang, P.; Song, Y.; Ohkoshi, S.; Hashimoto, K.; You, X. Z. *Dalton Trans.* **2008**, 2103–2106. (e) Wang, Z. X.; Wei, J.; Li, Y. Z.; Guo, J. S.; Song, Y. *J. Mol. Struct.* **2008**, *875*, 198–204. (f) Zhou, H.; Chen, Y. Y.; Yuan, A. H.; Shen, X. P. *Inorg. Chem. Commun.* **2008**, *11*, 363–366. (g) Zhou, H.; Yuan, A. H.; Shen, X. P.; Chen, Y. Y.; Price, D. J.; Kepert, C. J. *Inorg. Chem. Commun.* **2007**, *10*, 940–943. (h) Chen, Y. Y.; Zhou, H.; Shen, X. P.; Lu, H. F.; Yuan, A. H. *J. Mol. Struct.* **2007**, *839*, 64–68. (i) Yuan, A. H.; Zhou, H.; Chen, Y. Y.; Shen, X. P. *J. Mol. Struct.* **2007**, *826*, 165–169. (j) Wang, Z. X.; Li, X. L.; Wang, T. W.; Li, Y. Z.; Ohkoshi, S.; Hashimoto, K.; Song, Y.; You, X. Z. *Inorg. Chem.* **2007**, *46*, 10990–10995. (k) Lim, J. H.; Kang, J. S.; Kim, H. C.; Koh, E. K.; Hong, C. S. *Inorg. Chem.* **2006**, *45*, 7821–7827. (l) You, Y. S.; Yooh, J. H.; Lim, J. H.; Kim, H. C.; Hong, C. S. *Inorg. Chem.* **2005**, *44*, 7063–7069. (m) Korzeniak, T.; Stadnicka, K.; Peka, R.; Baanda, M.; Tomala, K.; Kowalski, K.; Sieklucka, B. *Chem. Commun.* **2005**, 2939–2941.

(14) (a) Zhang, W.; Wang, Z. Q.; Sato, O.; Xiong, R. G. *Cryst. Growth Des.* **2009**, *9*, 2050–2053. (b) Wang, Z. X.; Zhang, P.; Shen, X. F.; Song, Y.; You, X. Z.; Hashimoto, K. *Cryst. Growth Des.* **2006**, *6*, 2457–2462.

(15) (a) Podgajny, R.; Bałanda, M.; Sikora, M.; Borowiec, M.; Spałek, L.; Kapusta, C.; Sieklucka, B. *Dalton Trans.* **2006**, 2801–2809. (b) Korzeniak, T.; Stadnicka, K.; Rams, M.; Sieklucka, B. *Inorg. Chem.* **2004**, *43*, 4811–4813.

(16) Podgajny, R.; Nitek, W.; Rams, M.; Sieklucka, B. *Cryst. Growth Des.* **2008**, *8*, 3817–3821.

(17) (a) Typilo, I. V.; Sereda, O. A.; Stoeckli-Evans, H.; Gladyshevskii, R. E.; Semenyshyn, D. I. *Rus. J. Coord. Chem.* **2009**, *35*, 920–924. (b) Typilo, I. V.; Sereda, O. A.; Semenyshyn, D. I.; Stoeckli-Evans, H.; Gladyshevskii, R. E. *Pol. J. Chem.* **2009**, *83*, 339–344. (c) Sereda, O. A.; Stökli-Evans, G.; Typilo, I. V.; Semenyshyn, D. I.; Gladyshevskii, R. E. *Rus. J. Coord. Chem.* **2009**, *35*, 15–18. (d) Ma, S. L.; Ren, S.; Ma, Y.; Liao, D. Z. *J. Chem. Sci.* **2009**, *121*, 421–427. (e) Ma, S. L.; Ren, S. *J. Inorg. Organomet. Polym.* **2009**, *19*, 382–388. (f) Chelebaeva, E.; Larionova, J.; Guari, Y.; Ferreira, R. A. S.; Carlos, L. D.; Paz, F. A. A.; Trifonov, A.; Guérin, C. *Inorg. Chem.* **2009**, *48*, 5983–5995. (g) Tanase, S.; Evangelisti, M.; de Jongh, L. J.; Smits, J. M. M.; de Gelder, R. *Inorg. Chim. Acta* **2008**, *361*, 3548–3554. (h) Tanase, S.; de Jongh, L. J.; Prins, F.; Evangelisti, M. *ChemPhysChem* **2008**, *9*, 1975–1978. (i) Ma, S. L.; Ma, Y.; Liao, D. Z.; Yan, S. P.; Jiang, Z. H.; Wang, G. L. *Chinese J. Inorg. Chem.* **2008**, *24*, 1290–1293. (j) Chelebaeva, E.; Larionova, J.; Guari, Y.; Ferreira, R. A. S.; Carlos, L. D.; Paz, F. A. A.; Trifonov, A.; Guérin, C. *Inorg. Chem.* **2008**, *47*, 775–777. (k) Przychodzeń, P.; Peka, R.; Lewiński, K.; Supel, J.; Rams, M.; Tomala, K.; Sieklucka, B. *Inorg. Chem.* **2007**, *46*, 8924–8938. (l) Prins, F.; Pasca, E.; de Jongh, L. J.; Kooijman, H.; Spek, A. L.; Tanase, S. *Angew. Chem., Int. Ed.* **2007**, *46*, 6081–6084. (m) Kosaka, W.; Hashimoto, K.; Ohkoshi, S. *Bull. Chem. Soc. Jpn.* **2007**, *80*, 2350–2356. (n) Wang, Z. X.; Shen, X. F.; Wang, J.; Zhang, P.; Li, Y. Z.; Nfor, E. N.; Song, Y.; Ohkoshi, S.; Hashimoto, K.; You, X. Z. *Angew. Chem., Int. Ed.* **2006**, *45*, 3287–3291. (o) Tanase, S.; Prins, F.; Smits, J. M. M.; de Gelder, R. *CrystEngComm* **2006**, *8*, 863–865. (p) Przychodzeń, P.; Lewiński, K.; Peka, R.; Baanda, M.; Tomala, K.; Sieklucka, B. *Dalton Trans.* **2006**, 625–628. (q) Ikeda, S.; Hozumi, T.; Hashimoto, K.; Ohkoshi, S. *Dalton Trans.* **2005**, 2120–2123. (r) Hozumi, T.; Ohkoshi, S.; Arimoto, Y.; Seino, H.; Mizobe, Y.; Hashimoto, K. *J. Phys. Chem. B* **2003**, *107*, 11571–11574.

(18) (a) Culp, J. T.; Natesakhawat, S.; Smith, M. R.; Bittner, E.; Matranga, C.; Bockrath, B. *J. Phys. Chem. C* **2008**, *112*, 7079–7083. (b) Culp, J. T.; Smith, M. R.; Bittner, E.; Bockrath, B. *J. Am. Chem. Soc.* **2008**, *130*, 12427–12434.

(19) Bok, L. D. C.; Leipoldt, J. G.; Basson, S. S. *Z. Anorg. Allg. Chem.* **1975**, *415*, 81–83.

Table 1. Crystallographic Data and Refinement Details for **1**

complex	**1**
chemical formula	$C_{10}H_{10}N_9O_4TbW$
formula weight	663.04
crystal system	orthorhombic
space group	*Cmca*
a	16.436(5) Å
c	14.226(4) Å
c	14.866(4) Å
α	90.00°
β	90.00°
γ	90.00°
V	3476.0(2) Å^3
Z	8
D_{calcd}	2.534 g cm^{-3}
μ	10.685 mm^{-1}
F(000)	2432
GOF on F^2	1.021
$R_1/\omega R_2$ [$I > 2\sigma(I)$]	0.0269/0.0656
$R_1/\omega R_2$ (all data)	0.0385/0.0689

A few block-shaped red crystals formed after 10 days at 40 °C. Yield: 48% based on $Tb(NO_3)_3 \cdot 6H_2O$. Elemental analysis calcd (%) for $C_{10}H_{10}N_9O_4TbW$: C, 18.12; H, 1.52; N, 19.01. Found: C, 18.88; H, 1.39; N, 18.71. Powdered samples of **1** were obtained as follows: A 0.20 mmol quantity of $[HN(n\text{-}C_4H_9)_3]_3[W(CN)_8] \cdot 4H_2O$ together with 0.20 mmol $Tb(NO_3)_3 \cdot 6H_2O$ were dissolved in acetonitrile (40 mL), and the resulting suspension **I** was stirred for 6 h. An excess pyrazine (0.60 mmol) was dissolved in acetonitrile (15 mL) to give solution **II**. Solution **II** was poured slowly into solution **I** at 40 °C, resulting in the formation of red powdered products after further stirring for 24 h. Yield: 56% based on $Tb(NO_3)_3 \cdot 6H_2O$. Elemental analysis calcd (%) for $C_{10}H_{10}N_9O_4TbW$: C, 18.12; H, 1.52; N, 19.01; found: C, 17.93; H, 1.61; N, 19.17. Powder XRD patterns of the samples are in good agreement with those simulated from single crystal data of **1** (Supporting Information, Figure S1), which reveals highly purified products have been obtained by the mixing method under heating.

General Procedures and Materials. Elemental analyses for C, H, and N were performed with a Perkin-Elmer 240C elemental analyzer. IR spectra were measured on a Nicolet FT 1703X spectrophotometer in the form of KBr pellets in the 4000−400 cm^{-1} region. Temperature-dependent Raman spectra were recorded in backscattering geometry using JY-T6400 tripe monochromator. The 785 nm light from an Ar^+ laser was focused onto the sample surface under nitrogen atmosphere. The temperature stability of the sample was controlled within 0.1 K (THMS600/HFS91). The scattered signal from the sample was detected by a charge-coupled device detection system. Powder XRD patterns of $Tb(H_2O)_5[W(CN)_8]$ were collected with CuK_α radiation using a Shimadzu XRD-6000 diffractometer equipped with Anton-Paar HTK 1200 stage for atmosphere and temperature control. Dehydration measurements of pentahydrate complex $Tb(H_2O)_5[W(CN)_8]$ were run under flowing dry N_2 with a heating rate of 1 °C/min. For rehydration measurements of tetrahydrate complex $Tb(H_2O)_4[W(CN)_8]$, the N_2 flow was saturated with water vapor by diverting the flow through a water bubbler. Thermal analyses were carried out at a ramp rate of 5 °C/min under a dry N_2 atmosphere using a TA Instruments Hi-Res TGA 2950 analyzer. All of the magnetization data were recorded on a Quantum Design MPMS-XL7 SQUID magnetometer. Variable-temperature magnetic susceptibility measurement were performed in an applied field of 100 Oe in the temperature range of 300−1.8 K. The molar magnetic susceptibilities were corrected for the diamagnetism estimated from Pascal's tables and for the sample holder by a previous calibration. Gas adsorption measurements were performed on a Micromeritics ASAP 2020 analyzer. Sample tubes of a known weight were loaded and sealed using a transeal.

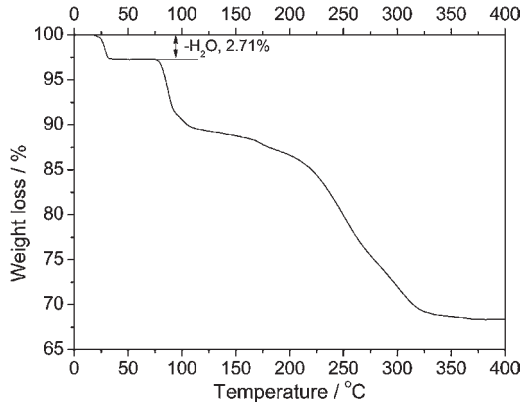

Figure 1. TG curve of $[Tb(H_2O)_5][W(CN)_8]$.

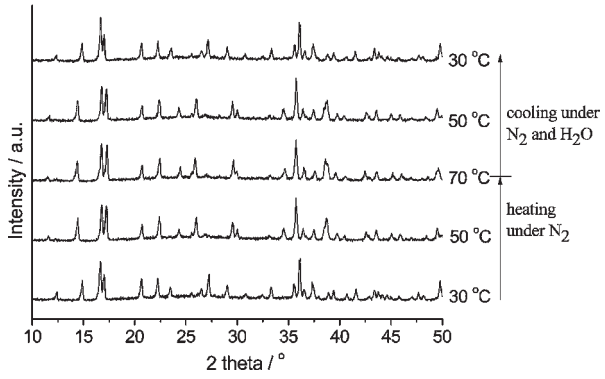

Figure 2. In situ variable-temperature powder XRD patterns of $Tb(H_2O)_5[W(CN)_8]$ with desorption and resorption of one coordinated water molecule.

Samples were degassed at 20 °C for 12 h, until the outgas rate was no more than 1 mTorr min^{-1}. The degassed sample and sample tube were weighed and then transferred back to the analyzer (with the transeal preventing exposure of the sample to air after degassing). The outgas rate was again confirmed to be less than 1 mTorr min^{-1}. Samples were maintained at constant temperature by immersion in a liquid nitrogen bath (77 K). UHP grade N_2 and H_2 (99.999%) gases were used for all measurements.

Crystallographic Data Collection and Structure Determination. Diffraction data for **1** was collected on a Bruker Smart APEX diffractometer equipped with MoKα (λ = 0.71073 Å) radiation. Diffraction data analysis and reduction were performed within SMART, SAINT, and XPREP.[20] Correction for Lorentz, polarization, and absorption effects were performed within SADABS.[21] Structures were solved using Patterson method within SHELXS-97[22] and refined using SHEwillLXL-97.[23] All non-hydrogen atoms were refined with anisotropic thermal parameters. The H atoms of pyrazine ligands were calculated at idealized positions with C−H = 0.93 Å and included in the refinement in a riding mode with U_{iso} for H assigned as 1.2 times U_{eq} of the attached atoms. The H atoms bound to coordinated water molecule were located from difference maps and refined as riding (O−H = 0.96 Å), with $U_{iso}(H) = 1.2U_{eq}(O)$. The crystallographic data and experimental details

(20) Bruker. *SMART, SAINT and XPREP: Area Detector Control and Data Integration and Reduction Software*; Bruker Analytical X-ray Instruments Inc.: Madison, WI, 1995.

(21) Sheldrick, G. M. *SADABS: Empirical Absorption and Correction Software*; University of Göttingen: Göttingen, Germany, 1999.

(22) Sheldrick, G. M. *SHELXS-97: Programs for Crystal Structure Solution*; University of Göttingen: Göttingen, Germany, 1997.

(23) Sheldrick, G. M. *SHELXL-97: Programs for the Refinement of Crystal Structures*; University of Göttingen: Göttingen, Germany, 1997.

Scheme 1. Formation Mechanism of **1**

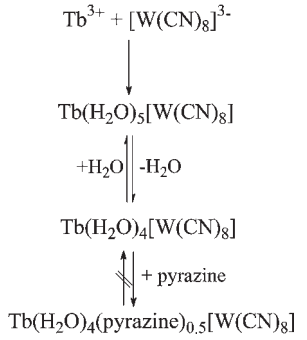

for structural analyses of **1** are summarized in Table 1. Selected bond lengths and angles are listed in Supporting Information, Table S1.

Results and Discussion

Synthetic Strategy and Crystal Formation Mechanism. It is notable that the temperature plays a crucial role for the formation of **1**, which can not be obtained at temperatures lower than ~33 °C. Only the 2D complex $[Tb(H_2O)_5][W(CN)_8]$ was formed below this temperature, which has been confirmed by powder X-ray diffraction (XRD) analysis (Supporting Information, Figure S2). Thermogravimetric (TG) analysis and variable-temperature powder XRD measurements were employed to clarify the mechanism of crystal formation. For the neutral precursor $[Tb(H_2O)_5][W(CN)_8]$, TG result (Figure 1) showed that the well-pronounced weight loss of 2.71% from 19 to 33 °C corresponded to the release of one coordinated water molecule (2.81%), accompanied by the phase transformation from $[Tb(H_2O)_5][W(CN)_8]$ to $[Tb(H_2O)_4][W(CN)_8]$ and the change in color from orange to purple. It should be mentioned that this process of phase transformation is reversible, which has been confirmed by variable temperature powder XRD experiments (Figure 2 and Supporting Information, Figure S3). No further weight loss was observed between 33 and 77 °C, above which the framework $Tb(H_2O)_4W(CN)_8$ collapsed.

Thus, the solution chemistry of the formation of **1** may be roughly elucidated as follows (Scheme 1): At temperatures below ~33 °C, the Tb ion center in $Tb(H_2O)_5W(CN)_8$ adopted a nine-coordinated monocapping square antiprism geometry, {TbO5N4}, and then began to transform to an eight-coordinated geometry {TbO4N4} in $Tb(H_2O)_4W(CN)_8$ upon heating. The transformation was complete, and pure $Tb(H_2O)_4W(CN)_8$ was obtained at ~33 °C. So there is one additional coordination site available for each Tb center in $Tb(H_2O)_4W(CN)_8$ at this temperature. In the presence of excess pyrazine, this feature allows the nitrogen atoms of pyrazine with the two ends having the same geometry to coordinate to Tb center. As a result, the coordination geometry of Tb changed again to a nine-coordinated geometry {TbO4N5}, resulting in a 3D inorganic−organic hybrid complex, **1**. TG results (Supporting Information, Figure S4) of **1** showed that the weight loss of 4.23% in the range from 18 to 170 °C was lower significantly than the theoretical value of the loss of the coordinated pyrazine (6.04%), which can be attributed to the partial loss of pyrazine ligands. Upon further heating, the framework collapsed, as shown by the absence of CN adsorption peaks at 200 °C in the Raman spectra (Supporting, Figure S5).

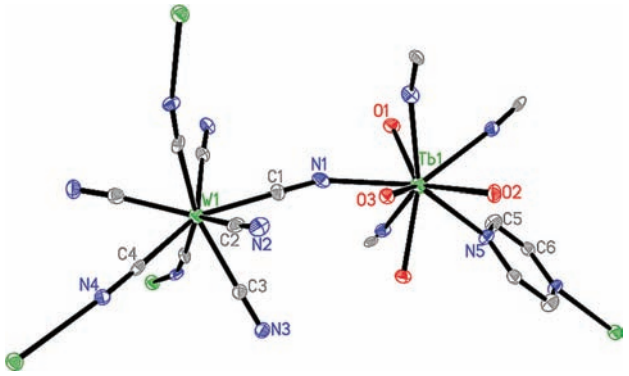

Figure 3. ORTEP diagram of **1**, showing the 30% probability thermal motion ellipsoid. Hydrogen atoms have been omitted for clarity. Symmetry codes: (iii) $-x+1, y, z$; (iv) $x-1/2, y-1/2, z$; (v) $-x+3/2, y-1/2, z$; (vi) $-x+3/2, y, -z+1/2$.

In addition, powder XRD patterns (Supporting Information, Figure S6) of the complex Nd-pyrazine-W obtained using the similar synthetic method are consistent with those simulated from single-crystal data of **1**, which indicates that the above building-block method is universal potentially for 2D layered Ln−M (M = Mo, W) system. Further research is in progress.

IR and Raman Spectra. IR spectrum of **1** exhibits two strong peaks at ~2172 and ~2159 cm^{-1} (Supporting Information, Figure S7). Terminal cyano ligands in $[W(CN)_8]^{3-}$ generally exhibit sharp, very intense bands in the region 2130−2170 cm^{-1}, while bridged cyano ligands shift to higher frequencies.[24] Therefore, a very strong band at ~2159 cm^{-1} is reasonably assigned to the terminal cyano stretching vibration. The very strong peak at ~2172 cm^{-1} confirms the predominant existence of the bridging cyano groups, indicating the formation of $Tb^{III}-NC-W^{V}$ bridges. In addition, the incorporation of pyrazine into **1** is detected by the presence of some sharp absorption bands below 1500 cm^{-1}. The similar behavior was observed from the recorded Raman spectra (Supporting Information, Figure S8).

Crystal Structure. Single-crystal X-ray structural analysis (Table 1) revealed that the asymmetric unit of **1** is composed of one $[Tb(H_2O)_4(pyrazine)_{0.5}]^{3+}$ cation and one $[W(CN)_8]^{3-}$ anion as shown in Figure 3. The eight-coordinated W center adopts a slightly distorted dodecahedron (Supporting Information, Figure S9), where four CN groups in $[W(CN)_8]^{3-}$ are bridged to Tb^{3+} centers and the other CN groups are terminal. The average values of W−C and C−N bond distances are 2.161 Å and 1.146 Å, respectively, while the W−C−N angles are nearly linear with a maximum deviation from linearity of 4.8° (Supporting Information Table S1). The coordination environment of W center is typical for the $[W(CN)_8]^{3-}$-based complexes.[10j,17m] The Tb center exhibits a nine-coordinated environment with four cyanonitrogens, one nitrogen atom from pyrazine ligand, and four oxygen atoms from water molecules. The coordination geometry around Tb is a slightly distorted tricapped trigonal prism with the capping position occupied by O3, $N4^{iv}$, and $N4^{v}$

(24) Kiernan, P. M.; Griffith, W. P. *J. Chem. Soc., Dalton Trans.* **1975**, 2489–2494.

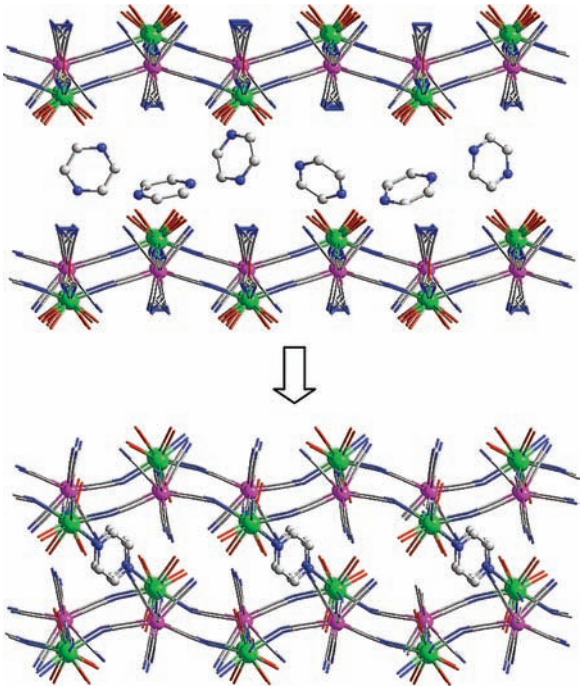

Figure 4. 2D-Corrugated layers[17f] further pillared by pyrazine ligands in the presence of heat, resulting in the formation of a 3D heterometallic network of **1**.

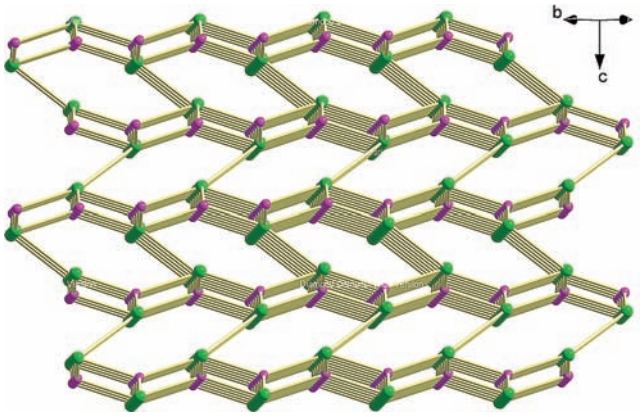

Figure 5. Topological representation of the 3D framework of **1**.

(symmetry codes (iv) $x - 1/2, y - 1/2, z$; (v) $-x + 3/2, y - 1/2, z$.) (Supporting Information, Figure S9), in which the mean Tb−N and Tb−O bond distances are 2.520 Å and 2.463 Å, respectively. Because of the large ionic radii of the lanthanide(III) centers, the cyanide bridges are exceptionally long and the Tb−N−C bonds are strongly bent with the angles ranging from 160.1° to 167.1°.

Thus, the Tb^{3+} and the $[W(CN)_8]^{3-}$ units are linked in alternating fashion in the *ab* crystallographic plane, resulting in an infinite 2D corrugated layers (Supporting Information, Figure S10a), which is practically composed of 12-membered $Tb_2W_2(CN)_4$ squares with the Tb(III) and W(V) atoms occupying the vertexes of the squares. The side view of the 2D corrugated layer is shown in Supporting Information, Figure S10b. It is noteworthy that the resulting 2D cyano-bridged Tb−W layers are ideally stacked in an ABAB fashion along the *c* axis. The linear bis-monodentate pyrazine ligands acting as pillars link

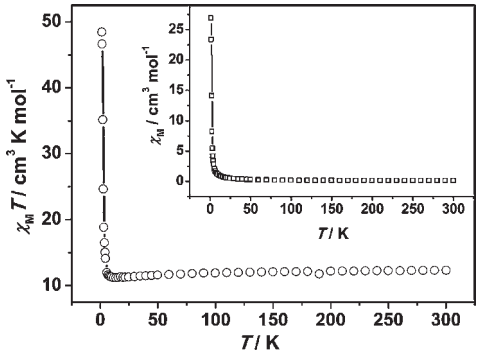

Figure 6. Temperature dependence of $\chi_M T$ (○) and χ_M (□) measured at 100 Oe. The solid lines are only guides for the eyes.

adjacent layers along the *c* axis to form an extended 3D open framework (Figure 4, Figure 5). To the best of our knowledge, only two examples of 3D organic−inorganic hybrid networks obtained from octacyanometallates (IV, V) and lanthanide ions, $[Ln^{III}(mpca)_2(H_2O)(CH_3OH)Ln^{III}(H_2O)_6W^{IV}(CN)_8]\cdot nH_2O$ (Ln = Eu, Nd)[17o] And **1** is the first structural example of 3D cyanide-based complexes including lanthanide ions and octacyanotungstate(V) group. As a result, pillared ligands pyrazine separate consecutive $\{Tb(H_2O)_4[W(CN)_8]\}_n$ layers by ~7.444 Å (W···W distance), which is slightly longer than the one (7.163 Å) in the neutral layer $Tb(H_2O)_5W(CN)_8$.[17f] In this case, the pillared ligands tilt away from the perpendicular, resulting in a condensed structure with low porosity. The unit cell contains no residual solvent accessible area calculated using the PLATON software taking into account the van der Waals radii of atoms.[25] The condensed structure has also been confirmed by the low significantly gas uptake (Supporting Information, Figure S11).

Magnetic Properties. The temperature dependence of the magnetic susceptibility of **1** was performed on a Quantum Design MPMS SQUID magnetometer with a 100 Oe applied field in the temperature range 1.8−300 K. The plots of $\chi_M T$ versus T and χ_M versus T are given in Figure 6. The observed $\chi_M T$ value per TbW unit at 300 K of 12.24 cm^3 K mol^{-1} slightly higher than the expected spin-only value of 12.19 cm^3 K mol^{-1} for an uncoupled spin system (one Tb^{III} ion in the $^7F_6$ ground state with $g_{Tb} = 3/2$, one $S_W = 1/2$ with $g_W = 2.0$). Upon cooling, the $\chi_M T$ value slightly decreases to a minimum value of 11.11 cm^3 K mol^{-1} at 12 K, and then increases sharply, reaching a maximum value of 48.39 cm^3 K mol^{-1} at 1.8 K. The initial decrease may be attributed to the thermal depopulation of the Stark levels of the terbium(III) $^7F_6$ ground state.[17f,j,l] The abrupt increase of $\chi_M T$ at low temperature is characteristic of the ferromagnetic correlation, which can be ascribed to two possible reasons: (1) the noncancellation of the antiferromagnetically coupled inequivalent Tb^{III} and W^V spins and (2) the ferromagnetically coupled Tb^{III} and W^V spins overcoming the depopulation of the Stark levels of Tb^{III} ion. Previously, Chelebaeva et al. reported that the 2D layered complexes $Tb(H_2O)_5[M(CN)_8]$ (M = Mo, W) exhibit ferromagnetic interactions based on the temperature dependences of $1/\chi_M$ fitted with the Curie−Weiss law above 50 K.[17f,j]

(25) Spek, A. L. *J. Appl. Crystallogr.* **2003**, 7–13.

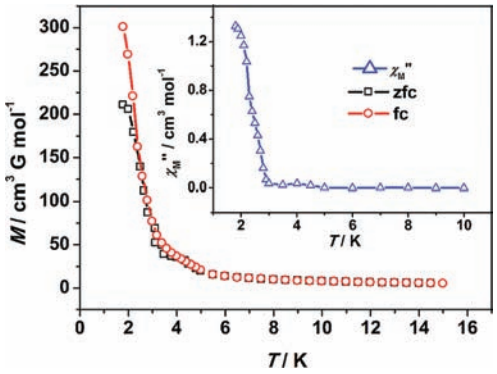

Figure 7. zfc and fc measurements of **1**. Inset is the out-of-phase susceptibility by ac measurements of **1** in Hdc = 0, Hac = 5 Oe, and f = 10 Hz.

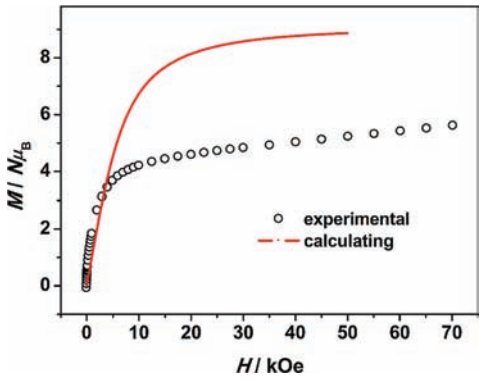

Figure 8. Field dependence of the magnetization performed at 1.8 K for **1**. The theoretical value of the saturation magnetization for ferromagnetic and antiferromagnetic interactions between Tb^{III} and W^{V} magnetic ions are equal to 6 μ_B and 4 μ_B, respectively.

From 12 to 1.8 K, $\chi_M T$ spans about 40 cm^3 K mol^{-1}, suggesting the occurrence of long-range ordering in **1**.

The further evidence can be obtained from the alternating current and direct current magnetic properties in low temperatures and low fields. Magnetization in 10 Oe after zero-field cool (zfc) and subsequent field cool (fc) are irreversible and bifurcated at ~2.5 K (Figure 7), indicating the formation of magnetic domains in **1**. Below the corresponding temperature, an observed abrupt increase of the out-of-phase susceptibility in ac measurements also indicates the long-range magnetic ordering in **1** (inset of Figure 7; in-phase of ac measurement is shown in Supporting Information, Figure S12). The phenomenon of the magnetic ordering has been also observed in the 2D layered complexes $M(H_2O)_5M'(CN)_8$ (M = Sm, Tb, Gd; M′ = Mo, W).[17f,j]

The field dependence of the magnetization measured at 1.8 K in the applied field 0−70 kOe is shown in Figure 8. The magnetization increases very rapidly in low field reaching 3.66 Nμ_B in 5 kOe, and gradually increases above this field to 5.61 Nμ_B in 70 kOe. Clearly, the magnetization does not reach saturation in 70 kOe and is much lower than 10 Nμ_B, on the basis of the noninteracting ions of [TbW] unit. This behavior has been found in other lanthanide complexes,[17k,26] because the effective spin of lanthanide ions is very small for the depopulation of the Stark levels at low temperature. For the 2D layered complexes $Tb(H_2O)M(CN)_8$ (M = Mo, W), the field dependence of the magnetization at 1.8 K has shown the magnetization data of 5.91 and 5.96 μ_B at 50 kOe for TbMo and TbW, respectively, which are expected for ferromagnetic interaction between Tb^{III} and W^{V} ions (6 μ_B) assuming a spin of S = 1/2 with an isotropic g factor (g = 2) for the W^{V} ion, and an effective spin of S = 1/2 with strong uniaxial Ising-type anisotropy of the g tensor ($g_{\|}$ = 10 and $g_{\perp}$ = 0) for the Tb^{III} magnetic moment.[17f] Similarly, we found that the experimental magnetization data of 5.61 μ_B at 70 kOe for our sample **1** was slightly lower than the value of 6 μ_B, indicating the presence of the ferromagnetic interaction between Tb^{III} and W^{V} ions (Figure 8).

Conclusions

In summary, the self-assembly of neutral layers $Tb(H_2O)_5[W(CN)_8]$ and the pillared ligand pyrazine has resulted in a novel 3D heterometallic complex $Tb(H_2O)_4(pyrazine)_{0.5}[W(CN)_8]$ (**1**), which marks the first structural pattern using neutral 2D layers as building block and the first 3D complex with Ln^{III}-$[W^{V}(CN)]_8$ found in octacyanometallate-based system. From magnetic susceptibility data, we find an ferromagnetic interaction between Tb^{III} and W^{V} ions. The possible formation mechanism is proposed. We believe that such a novel and effective building-block methodology will provide a new attractive path forward in developing functionalities of 3D octacyano- and lanthanide-based system and may provide an opportunity to obtain 3D magnet in 4f-5d assembly. The further research in our laboratory will include: (i) a systematic study varying the type of lanthanide metal ion and also replacing W^{V} by Mo^{V}, (ii) investigation into luminescent properties of such 3D system, and (iii) longer pillar ligands employed to construct porous frameworks having potential applications in gas storage field.

Acknowledgment. This work was supported by the University Natural Science Foundation of Jiangsu Province (No. 07KJB150030, China) and National Natural Science Foundation of China (Nos. 20773107, 20631030, and 20771057). The authors thank Cameron J. Kepert (The University of Sydney, Australia) for synthesis, X-ray diffraction, and thermogravimetric measurements of $Tb(H_2O)_5W(CN)_8$.

Supporting Information Available: X-ray crystallographic data in CIF format of complex **1**, additional tables, and figures. This material is available free of charge via the Internet at http://pubs.acs.org.

(26) Tang, J.; Hewitt, I.; Madhu, N. T.; Chastanet, G.; Wernsdorfer, W.; Anson, C. E.; Benelli, C.; Sessoli, R.; Powell, A. K. *Angew. Chem., Int. Ed.* **2006**, *45*, 1729–1733.